Inorganic Chemistry

Article

pubs.acs.org/IC

Novel Isopolyoxotungstate $[H_2W_{11}O_{38}]^{8-}$ Based Metal Organic Framework: As Lewis Acid Catalyst for Cyanosilylation of Aromatic Aldehydes

Qiuxia Han,*[,†] Xueping Sun,[‡] Jie Li,[†] Pengtao Ma,[†] and Jingyang Niu*[,†]

[†]Institute of Molecular and Crystal Engineering, School of Chemistry and Chemical Engineering, Henan University, Kaifeng 475004, People's Republic of China

[‡]Department of Environmental Engineering and Chemisty, Luoyang Institute of Science and Technology, Luoyang 471023, People's Republic of China

Supporting Information

ABSTRACT: A novel polyoxometalate-based metal organic framework (POMOF) constructed from isolated isopolyoxotungstate $[H_2W_{11}O_{38}]^{8-}$ cluster, $\{[Cu_2(bpy)(H_2O)_{5.5}]_2[H_2W_{11}O_{38}]\cdot 3H_2O\cdot 0.5CH_3CN\}$ (**1**, where bpy = 4,4′-bpydine), has been synthesized under solvothermal conditions and charaterized by elemental analysis, infrared spectroscopy, and single-crystal X-ray diffraction. In **1**, $\{W_{11}\}$ clusters are alternately linked by two $[Cu(2)(H_2O)_{1.5}(O_t)_3(N)]^{2+}$ cations in an unexpected end-to-end fashion leading to a one-dimensional (1D) chain. Adjacent 1D chains are linked through Cu(1)−bpy−Cu(2) in an opposite direction to form a two-dimensional (2D) wavelike sheet along the *ab* plane. These 2D sheets are further stacked in a parallel fashion giving rise to the 1D channels with copper(II) cations aligned in the channels. The resulting POMOF acted as a Lewis acid catalyst through a heterogeneous manner to prompt cyanosilylation with excellent efficiency.

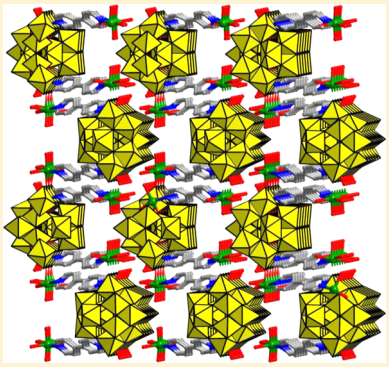

INTRODUCTION

Polyoxometalate-based metal organic frameworks (POMOFs), with infinite networks constructed from polyoxometalates (POMs) that act as either templates or inorganic connecting nodes, and metal organic frameworks (MOFs), have attracted increasing attention and developed rapidly as a new class of organic−inorganic hybrid solids over recent years.[1,2] The unique physical and chemical properties and diverse coordination modes of POMs together with the diversity of organic linkers provide a stimulus to the synthesis of multifunctional POMOFs. Recently, POMOFs have revealed broad prospects in applications as solid acids and oxidation catalysts and become attractive candidates as heterogeneous catalysts because of their size- and shape-selective restriction abilities through elaborately fine-tuned channels or pores.[3,4] In particular, the introduction of POMs into MOFs at the molecular scale will contribute to the complexity, stability, and corresponding functionality of the resulting POMOFs, thus endowing them with new features and multiple functionalities distinctively different from the POMs or MOFs alone.[5,6]

Polyoxotungstates (POTs) are a large class of well-known polynuclear tungstate−oxo clusters with an unmatched structure variety and excellent thermal and oxidative stability properties, representing one of the diverse building blocks for the construction of functional POMOFs.[7−9] Two main types of POTs are known: the *hetero*-POTs and the *iso*-POTs. Hetero-POTs with the general formula $[X_pW_qO_y]^{n-}$ (where X = P^V, As^V, Si^{IV}, Ge^{IV}), especially the archetypal and lacunary Keggin $[XW_{12}O_{40}]^{n-}$ and Wells−Dawson $[X_pW_{18}O_y]^{n-}$ (p = 1 or 2, m = 60 or 62) anions, have gone through extensive development and were used to construct POMOFs with excellent catalytic efficiency in a heterogeneous manner.[10−16] Compared to the popular hetero-POT-based POMOFs, only a few examples of POMOFs consisting of iso-POTs with the general formula $[W_qO_y]^{n-}$ were reported,[17,18] which presents a great opportunity to launch explorations on their possibility to be reliably utilized as a set of transferable building blocks in the formation of new materials.

Among the reported iso-POTs, $[W_{11}O_{38}]^{10-}$ (abbreviated as $\{W_{11}\}$) is a fundamental building block because it has the potential to be degraded to a $[H_2W_8O_{32}]^{14-}$ cluster or be aggregated to larger clusters.[19−22] Cronin and co-workers reported several appealing iso-POT clusters generated from pure iso-POT $\{W_{11}\}$ clusters, such as $[H_4W_{22}O_{74}]^{12-}$, $[H_{10}W_{34}O_{116}]^{18-}$, and $[H_{12}W_{36}O_{120}]^{12-}$. $[H_4W_{22}O_{74}]^{12-}$ consisted of two $\{W_{11}\}$ subunits fused via two μ_2-oxo bridges in a trans fashion; $[H_{10}W_{34}O_{116}]^{18-}$ was built from two $\{W_{11}\}$ clusters connecting with one $[H_2W_{12}O_{42}]^{10-}$ $\{W_{12}\}$ cluster through two μ_2-oxo bridges in a trans fashion, giving an expanded §-like architecture;[20] and $[H_{12}W_{36}O_{120}]^{12-}$ displayed an overall triangular shaped cluster constructed from three $\{W_{11}\}$ clusters linking together with three $\{W_1\}$ bridges sharing four bridging oxo ligands in the equatorial plane.[21] Then, they

Received: March 1, 2014
Published: June 6, 2014

   dx.doi.org/10.1021/ic5004879 | *Inorg. Chem.* 2014, 53, 6107−6112

reported a quadrangular shaped superstructure $[H_{10}Te^{VI}_2W_{58}O_{198}]^{26-}${$W_{58}$} cluster that consisted of two tellurium-centered Dawson clusters and two {W_{11}} clusters.[22] This fact clearly indicated that the {W_{11}} cluster is very labile and more inclined to assemble by W−O−W bonds. In addition, Kortz and co-workers further extended the structural motif and discovered a new member of the iso-POT family based on the {W_{22}} architecture, such as $[Ln_2(H_2O)_{10}W_{22}O_{71}(OH)_2]^{8-}$ (Ln = lanthanide), in which the {W_{22}} cluster acted as a tridentate ligand coordinated to two Ln^{3+} ions.[23] Yao also reported a similar structure $Ca_2(H_2O)_{12}\{Ca_4(H_2O)_{18}[H_2W_{11}O_{37}]_2\}\cdot 20H_2O$, in which the {$W_{22}$} decorated six calcium ions.[24] Subsequently, Kortz reported the first example of polyanion, $[Ln_2(H_2O)_{10}W_{28}O_{93}(OH)_2]^{14-}$, which was constructed by two $\{Ln(H_2O)_n\}^{3+}$ groups linking two isolated {W_{11}} clusters and a hexatungstate {W_6} fragment.[25]

As illustrated previously, most of the reported iso-POTs based on {W_{11}} clusters were purely inorganic aggregations and synthesized in the conventional aqueous solution. However, the organic−inorganic hybrids containing isolated {W_{11}} cluster have not been reported. Because the {W_{11}} cluster possesses high charges, strongly basic oxygen surfaces and much more lacunary-like positions, we envisioned that the {W_{11}} cluster may be beneficial for coordination with more transition metal ions as multidentate ligand in the presence of organic ligand to form new POMOFs with multifunctionalities. Therefore, the present work is based on excellent past studies of the POMOFs in catalysis aspect, introducing a new strategy to broaden the application of POMOFs as heterogeneous catalysts for cyanosilylation of aromatic aldehydes. Using $[W_{10}O_{32}]^{4-}$ as starting material to react with Cu(II) cation and bpy under hydrothermal conditions resulted in a novel POMOF based on iso-POT {W_{11}} {$[Cu_2(bpy)(H_2O)_{5.5}]_2[H_2W_{11}O_{38}]\cdot 3H_2O\cdot 0.5CH_3CN$} (**1**; see Scheme 1). Unexpectedly, the {W_{11}} cluster first exists as an isolated unit rather than an aggregation and simultaneously coordinates with six Cu complex ions to display a new 2D framework. These 2D sheets are further stacked in a parallel fashion giving rise to the 1D channels with copper(II) ions aligned in the channels, which ensures the resulting well-defined POMOF **1** can act as a Lewis acid catalyst to prompt the cyanosilylation with excellent efficiency by interacting with guest molecules getting into the channels. Besides, catalyst **1** can be easily separated from product and reusable at least three times with only moderate loss of activity, which are considered advantages of this heterogeneous catalyst.

Scheme 1. Synthetic Procedure of 1, Showing the Rearrangement of Precursor $[W_{10}O_{32}]^{4-}$ and the 2D Framework Constructed by $[H_2W_{11}O_{38}]^{8-}$ Anions and Copper(II) Complexes.[a]

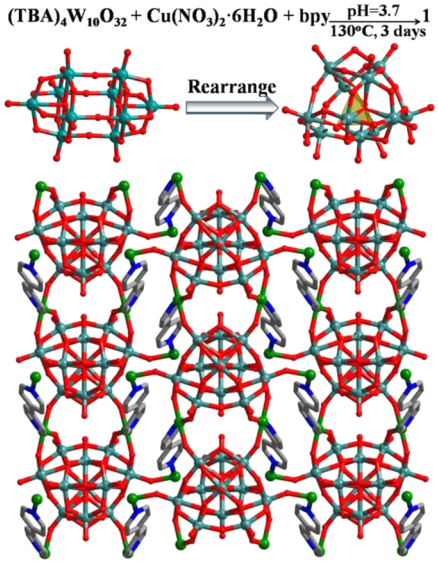

[a]Color legend: green, Cu^{2+}; gray, C; blue, N; red, O; teal, W. For the sake of clarity, the H atoms and coordinated H_2O molecules are omitted for clarity.

EXPERIMENTAL SECTION

General Methods and Materials. All reagents were commercially purchased and used without further purification. $(TBA)_4W_{10}O_{32}$ (where TBA = $[(C_4H_9)_4N]^+$) was prepared according to the literature and characterized by IR spectroscopy.[26] Elemental analyses (EA) of C, H, and N were performed on a Vario ELIII elemental analyzer. Inductively coupled plasma (ICP) of Cu and W analyses were performed on a Jarrel-Ash Model J-A1100 spectrometer. The infrared spectra (IR) were recorded from a sample powder palletized with KBr on a Nicolet170 SXFT-IR spectrometer over a range of 400−4000 cm^{-1}. Powder X-ray diffraction (PXRD) data were obtained on a Rigaku Model D/Max-2400 X-ray diffractometer with a sealed copper tube (λ = 1.54178 Å). ^1H NMR was measured on a Varian INOVA-400 spectrometer with chemical shifts reported in parts per million (ppm; in $CDCl_3$; tetramethylsilane (TMS) as internal standard).

*Synthesis of {$[Cu_2(bpy)(H_2O)_{5.5}]_2[H_2W_{11}O_{38}]\cdot 3H_2O\cdot 0.5CH_3CN$} (**1**).* Compound **1** was synthesized by the self-assembly approach under hydrothermal conditions: $(TBA)_4W_{10}O_{32}$ (65 mg, 0.02 mmol), $Cu(NO_3)_2\cdot 6H_2O$ (57.5 mg, 0.19 mmol), and bpy (8 mg, 0.05 mmol) were mixed in 3 mL of water and 3 mL of acetonitrile solution at pH 3.7. The resultant mixture was stirred for 6 h, then sealed in a 25 mL Teflon-lined autoclave, and maintained at 130 °C for 3 days. After cooling the autoclave to room temperature, green cubic single crystals were separated, washed with water, and air-dried. The crystals were obtained with a moderate yield of 40% based on $(TBA)_4W_{10}O_{32}$. EA and ICP (%). Calcd for $C_{21}H_{47.5}Cu_4N_{4.5}O_{52}W_{11}$: C 7.27, H 1.38, N 1.82, Cu 7.32, W 58.25;. Found: C 7.30, H 1.32, N 1.88, Cu 7.37, W 58.34. IR (KBr; ν): 3423 (br, s), 2927 (w), 2862 (w), 2281 (w) 1606 (s), 1542 (w), 1488 (w), 1412 (m), 1221 (w), 935 (s, W═O_t), 823 (s, W−O−W) cm^{-1}.

X-ray Crystallographic Analysis. The crystallographic data of **1** were collected on a Bruker SMART APEX CCD diffractometer with graphite-monochromated Mo Kα (λ = 0.71073 Å) using the SMART and SAINT programs.[27,28] The intensity data were corrected for Lorentz and polarization effects as well as for multiscan absorption. The structure was solved by direct methods and refined by full-matrix least-squares on F^2 using the SHELXTL-97 program package.[29] All of the non-hydrogen atoms except for partial crystal water and CH_3CN molecules were refined anisotropically in **1**. Positions of the hydrogen atoms attached to the carbon atoms were refined isotropically as a riding mode using the default SHELXTL parameters. The hydrogen atoms attached to water molecules were not located in **1**. Crystallographic data for **1** were summarized in Table 1. Selected bond lengths and angles of **1** are listed in Table S1 in the Supporting Information.

RESULTS AND DISCUSSION

Synthesis. Compound **1** was solvothermally prepared by reaction of $(TBA)_4W_{10}O_{32}$, $Cu(NO_3)_2\cdot 6H_2O$, and bpy in mixed water and acetonitrile with a yield of 40%. As we know, the formation of various structure types of POMs mainly depends on the pH value and the reaction temperature. The results showed that the pH value of the system varied over a range of 3.7−3.9, which was helpful for the formation of **1**. When at pH 4.3, a new organic−inorganic hybrid $[Zn(bpy\text{-}NH_2)_4(H_3O)_2]$-

dx.doi.org/10.1021/ic5004879 | Inorg. Chem. 2014, 53, 6107−6112

Table 1. Crystallographic Data and Structure Refinement for 1

parameter	1
empirical formula	$C_{21}H_{47.5}Cu_4N_{4.5}O_{52}W_{11}$
mol wt, M (g mol^{-1})	3471.53
crystal system	monoclinic
space group	$P2(1)/m$
a (Å)	10.008(1)
b (Å)	21.721(3)
c (Å)	14.825(2)
β (deg)	108.029(2)
V (Å^3)	3064.5(7)
Z	1
D_{calcd} (g cm^{-3})	3.729
T (K)	296(2)
reflcns collected/unique	14120/5522 [$R_{(int)}$ = 0.0433]
μ (mm^{-1})	22.016
F(000)	3042
GOF	1.009
$R_1{}^a$ ($I > 2\sigma(I)$)	0.0411
$R_{2w}{}^b$ ($I > 2\sigma(I)$)	0.1111
$R_1{}^a$ (all data)	0.0604
$R_{2w}{}^b$ (all data)	0.1187
diff peak and hole, eÅ^{-3}	2.986/−2.249

$^aR_1 = \sum||F_o| - |F_c||/\sum|F_o|$. $^bR_{2w} = [\sum w(F_o^2 - F_c^2)^2/\sum w(F_o^2)^2]^{1/2}$; $w = 1/[\sigma^2(F_o^2) + (xP)^2 + yP]$, $P = (F_o^2 + 2F_c^2)/3$, where $x = 0.0700$ and $y = 6.9018$ for **1**.

$[W_{10}O_{32}]\cdot 2H_2O$ was obtained, in which the $[W_{10}O_{32}]^{4-}$ structure was maintained.[30] When at pH 3.6, $[W_{10}O_{32}]^{4-}$ reacted with $Zn(NO_3)_2$ in the presence of bpy and formed a new POMOF, in which $[W_{10}O_{32}]^{4-}$ was reorganized into Keggin-type $[ZnW_{12}O_{40}]^{6-}$.[31] These results indicate the precursor $[W_{10}O_{32}]^{4-}$ tends to transform to iso-POT $[H_2W_{11}O_{38}]^{8-}$ or hetero-POT $[XW_{12}O_{40}]^{n-}$ (X = transition metal) during the course of the reaction, which benefited from the produced high temperature and pressure under solvothermal conditions that can make the reaction shift from the thermodynamic to the kinetic. In addition, the introduction of the rigid organic ligand bpy into this system is conducive to the stability of the formed POMOF. Therefore, the successful synthesis of **1** showed that this simple but very efficient strategy can offer an effective way to make novel multidimensional iso-POT frameworks.

Structural Description. Single-crystal structural determination reveals that the compound **1** crystallizes in a space group $P2(1)/m$ and consists of an iso-POT $[H_2W_{11}O_{38}]^{8-}$, four hexacoordinated copper cations ($[Cu(1)(H_2O)_4(O_t)(N)]^{2+}$ and $[Cu(2)(H_2O)_{1.5}(O_t)_3(N)]^{2+}$), three water molecules of crystallization, and a half molecule of CH_3CN (see Figure 1). The bond-valence sum (BVS) model clearly indicates that all of the tungsten atoms are in the +6 oxidation state and the copper atoms are in the +2 oxidation state, respectively.[32] Both of the two crystallographically independent Cu(II) ions in **1** adopt the distorted octahedral geometries. In $[Cu(1)(H_2O)_4(O_t)(N)]^{2+}$, the Cu(1) atom is defined by four oxygen atoms from coordinated water [Cu(1)−O_w, 1.986(6)−2.424(5) Å], one bridging oxygen atom from $\{W_{11}\}$ [Cu(1)−O(13), 1.971(4) Å], and one nitrogen atom from bpy [Cu(1)−N(1), 1.992(6) Å]. O(1W) and O(2W) occupy the axial positions of the elongated octahedron; other atoms build the equatorial plane. In $[Cu(2)(H_2O)_{1.5}(O_{POT})_3(N)]^{2+}$, the Cu(2) atom is defined by 1.5 water oxygen atoms (sof (site occupancy fraction) of O(9W) is 0.5) [Cu(2)−O_w, 1.866(13)−2.274(5) Å], three oxygen atoms from $\{W_{11}\}$[Cu(2)−O_{POT}, 1.912(4)−1.982(4) Å], and one nitrogen atom from bpy [Cu(2)−N(1), 1.983(5) Å].

Similar to the framework geometry of the $[H_4W_{11}O_{38}]^{6-}$ cluster reported by Lehmann and Fuchs,[33] the $\{W_{11}\}$ subunit in

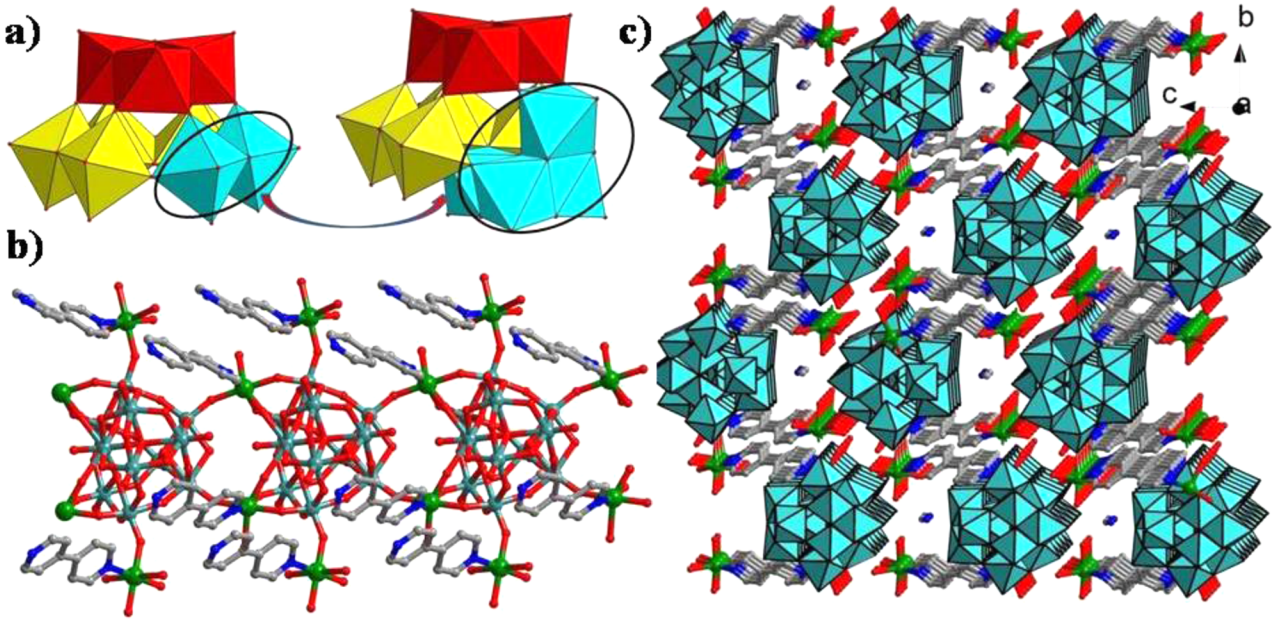

Figure 1. (a) Polyhedron representation of the $\{W_9\}$ trivacant lacunary Keggin anion and the $\{W_{11}\}$ adduct. (the heteroanion is omitted for clarity). To make a comparison between the iso-POT and hetero-POT, the different parts of the two structures are highlighted. (b) Ball-and-stick representations of the coordinated mode of $\{W_{11}\}$ and coordination environments of copper(II) ions. (c) Crystal structure of **1** showing the stacking pattern of the grid-like sheets and the 1D channels along the a axis. The H atoms and free H_2O molecules are omitted for clarity. Color legend: gray, C; blue, N; red, O; green, Cu^{2+}; teal, polyhedra $\{W_{11}\}$.

dx.doi.org/10.1021/ic5004879 | Inorg. Chem. 2014, 53, 6107−6112

1 is composed of four distinct fundamental groups: one $\{W_4O_{21}\}$ group formed from four edge-shared WO_6 octahedra connected through a μ_4-hydroxo, one $\{W_3O_{16}\}$ group formed from three edge-shared WO_6 octahedra connected through a μ_3-hydroxo bridge, and two $\{W_2O_{10}\}$ fragments, each formed from two edge-shared WO_6 which share corners on one side. The structure of $\{W_{11}\}$ can be seen as the derivative from the trivacant Keggin anion A-$[XW_9O_{34}]^{n-}$,[34] in which a tetrameric unit $\{W_4O_{16}\}$ displaces a dimeric unit $\{W_2O_{10}\}$ introducing asymmetry to the $\{W_{11}\}$ cluster (Figure 1a). All W centers have the distorted WO_6 octahedral coordination geometries, with one terminal O_t (average bond lengths of W−O_t, 1.728 Å) extending away from the cluster. Relevant W−O_a (central) bond distances vary from 2.182(3) to 2.318(3) Å (but both W(2)−O(3) and W(2)−O(3A) are 1.866(4) Å). The W−$O_{b,c}$ (bridging) bond distances range from 1.784(4) to 2.130(4) Å. Within the $\{W_{11}\}$ moiety, the four inner μ−O positions span a nearly regular {O4} tetrahedron (O···O distances, 2.754−2.996 Å). The μ_4-O and μ_3-O display the highest negative partial charges (BVS for the sites are 1.3 for O(2) and 1.5 for O(14), respectively.). Most interestingly, each $\{W_{11}\}$ cluster acts as a hexadentate ligand to coordinate with six copper complex cations nearly in a plane by the terminal or bridging oxygen atoms of a ring of six basal W positions. The $\{W_{11}\}$ fragment possesses much more negative charges, which may be beneficial for coordination with more TM ions as the multidentate ligand to form a new organic−inorganic framework. It is fact that the W═O_t bonds participated in coordination with copper were 0.026 Å (on average) longer than the other W═O_t bonds. While one or two metal centers coordinated with oxygen atoms of POM is a well-established structural paradigm for POMs,[35] a higher coordination number for a POM anion is very unusual. In 2003, the first example that a Keggin-type $[PV_2Mo_{10}O_{40}]^{5-}$ was bound to six $[Cu(H_2O)_4]^{2+}$ by the terminal oxygen atoms of a ring of six basal W positions was reported by Hill et al.[36] Then, Arumuganathan and Das reported a POV cluster anion, $[As_8V_{14}O_{42}(SO_3)]^{6-}$, with six surrounding lanthanum−aqua complex cations.[37]

As can be seen from Figure 1b, $\{W_{11}\}$ clusters are alternately linked by two $[Cu(2)(H_2O)_{1.5}(O_{POT})_3(N)]^{2+}$ cations in an unprecedented end-to-end fashion to form a 1D chain with the linkage mode of (-$\{W_{11}\}$−Cu(2)−$\{W_{11}\}$-). Adjacent 1D chains are linked through Cu(1)−bpy−Cu(2) in an opposite direction to form a 2D wave-like network along the *ab* plane (see Figure S3 in the Supporting Information). These 2D sheets are further stacked in a parallel fashion through the interactions between $\{W_{11}\}$ and the copper(II) centers giving rise to the 1D channels along the *a* axis with a cross-section of about 5.6 × 6.6 $Å^2$ (see Figure 1c). However, there are a few of the free H_2O and CH_3CN molecules occupying the pores of the channels. As we know, the solvents contained in MOFs can be removed by two common treatments. One is thermally assisted evacuation, and the other is liquid exchange of the encapsulated solvents such as dimethylformamide (DMF) and dimethylacetamide (DMAC) for lower boiling point solvents such as MeOH and tetrahydrofuran (THF) followed by a degas process or pore evacuation at moderate temperature.[38,39] Herein, the first treatment was adopted to extract the water and CH_3CN from the pores. As a result, channels of **1** were theoretically enlarged with the accessible pores from 160.4 to 429.6 $Å^3$ (from 5.2% to 14.0% of the unit cell volume), as calculated from PLATON analysis.[40] The water molecules occupy several coordination sites of copper(II) cations and potentially act as removable labile ligands, allowing for copper(II) to serve as the catalytically active sites interacting with the guest molecules that get into the channels.[41,42]

Although hetero-POTs have been extensively exploited to develop the organic−inorganic architectures, no organic−inorganic hybrids based on isolated $\{W_{11}\}$ clusters and transition metal complexes have been reported to date. To the best of our knowledge, except for a handful of pure inorganic iso-POT clusters related $\{W_{11}\}$ assembled by W−O−W bonds,[20−22] only one lanthanide-containing iso-POT $[Ln_2(H_2O)_{10}W_{28}O_{93}(OH)_2]^{14-}$ constructed by isolated $\{W_{11}\}$ clusters with $\{Ln(H_2O)_n\}^{3+}$ ions has been reported.[23] In **1**, $\{W_{11}\}$ acts as a lacunary POT cluster possessing four naked bridging oxygen connected with two copper complexes, resulting in a nontypical sandwich structure. It is particularly worth mentioning that the $\{W_{11}\}$ clusters are linked by two copper(II) complexes in an end-to-end fashion, while the reported dinuclear sandwiched hetero-POM are usually connected in a face-to-face way.[43] For example, $[Cu(en)_2H_2O]_2\{[Cu(en)_2][Cu(en)_2As^{III}As^{V}Mo_9O_{34}]\}_2\cdot 4H_2O$ is constructed from two $\{[Cu(en)_2][As^{III}As^{V}Mo_9O_{34}]\}^{4-}$ units and two $[Cu(en)_2]^{2+}$ complex cations via two O−Cu−O bridges in a trans fashion, which is analogous to $[H_4W_{22}O_{74}]^{12-}$.[20] The successful synthesis of **1** showed that $\{W_{11}\}$ cluster can act as a versatile inorganic unit for construction of POMOFs displaying diverse structural motifs and properties. Therefore, the systematic exploration of the $\{W_{11}\}$ system still remains a great challenge and further study is needed.

Powder XRD Characterization and IR Spectra. The powder XRD pattern for compound **1** is presented in Figure S1 in the Supporting Information. The very good correspondence between the calculated and the experimental patterns suggests the high purity of the bulk sample. This conclusion is in agreement with the results of the single-crystal X-ray analysis.

The IR spectrum of compound **1** displays characteristic stretching vibrations related to those seen in other species containing $[W_{11}O_{38}]^{10-}$[25] (see Figure S2 in the Supporting Information). The IR spectrum of **1** shows two very strong absorption peaks near 935 and 823 cm^{-1} that are assigned to the vibration of W═O_t and W−O−W of the iso-POT $\{W_{11}\}$ cluster, respectively. The broad peak at 3423 cm^{-1} is attributed to the characteristic vibration peak of H_2O. In addition, the vibration peaks from 1221 to 1606 cm^{-1} are indicative of the bpy ligand. The occurrence of these resonance signals confirms the presence of bpy and water molecules, which is in good agreement with the single-crystal structural analysis.

Catalysis. The cyanosilylation was carried out in the presence of POMOF **1** with a 1:2.4 mol ratio of the selected aromatic aldehydes and cyanotrimethylsilane in CH_3CN for 24 h at room temperature through a heterogeneous manner. The results summarized in Table 2 showed that the 2 mol % mole ratio loading of catalyst **1** (0.01 mmol) caused significant catalytic efficiency with conversion of up to about 98% of the 2-phenyl-2-(trimethylsilyloxy)acetonitrile corresponding to benzaldehyde. In addition, the removal of **1** by filtration after 12 h terminated the reaction, and the filtrate afforded only 9% additional conversion after being stirred at temperature for another 12 h. Solids of **1** could be easily isolated from the reaction suspension by a simple filtration alone and reused at least three times with moderate loss of activity (from 98.2% to 93.8% conversion; see Table S2 in the Supporting Information). The index of the PXRD pattern of the bulky sample that

dx.doi.org/10.1021/ic5004879 | *Inorg. Chem.* 2014, 53, 6107−6112

Table 2. Results for the Catalytic Cyanosilylation of Aldehydes in the Presence of 1[a]

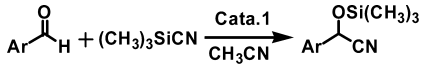

entry	Ar−	yield (%)[b]
1	phenyl	98.1
2	4-methoxyphenyl	89.3
3	1-naphthyl	87.8
4	2-naphthyl	88.0
5	3-formyl-1-phenylene-(3,5-di-*tert*-butylbenoate)	52.4

[a]Reaction conditions: $(CH_3)_3SiCN$, 1.2 mmol; aldehyde, 0.5 mmol; catalyst **1**, 0.01 mmol (2 mol %); CH_3CN, 2 mL; at room temperature under N_2 for 24 h. [b]The conversions were determined by ^1H NMR spectroscopy of crude products.

was collected after three runs of the catalytic reaction evidenced the maintenance of the crystallinity (see Figure S1 in the Supporting Information). These observations suggested that **1** is a true heterogeneous catalyst. The use of such a catalyst can be extended to other aromatic aldehyde substrates with comparable activity. Infrared spectroscopy of the catalyst **1** impregnated with a CH_3CN solution of benzaldehyde exhibited one broad C−O stretch at 1693.6 cm^{-1}. The ν(C−O) stretch had a red shift of 12.9 cm^{-1} from 1706.5 cm^{-1} of the free benzaldehyde (see Figure S2 in the Supporting Information). This experiment unambiguously demonstrated the absorbance of benzaldehyde and possible activation of the substrate by the unsaturated Cu(II) in the channels of **1**.

In contrast to the smooth reaction of substrates **1**−**4**, the cyanosilylation catalytic reaction in the presence of bulky aldehyde 3-formyl-1-phenylene-(3,5-di-*tert*-butylbenzoate) gave less than 52% of conversion under the same reaction conditions. Further adsorption experiments by immersing solids of **1** into a solution of substrate **5** also confirmed that substrate **5** was too large to be adsorbed in the channels of the POMOF.[44] The size selectivity of the substrate suggested that cyanosilylation indeed occurs in the channels of the POMOF, not on the external surfaces. The control experiments for cyanosilylation of benzaldehyde with free $Cu(NO_3)_2$ and $(TBA)_{12}[H_4W_{22}O_{74}]$ (prepared according to literature methods[20]) in a homogeneous manner gave 45.4% and 11% conversion, respectively, which are far lower than that of **1** in the heterogeneous manner. The higher conversion with **1** is possibly attributed to the suitable distribution of copper(II) and $\{W_{11}\}$ in the POMOF that provides effective contacts with substrates at the same time.

CONCLUSION

In summary, a novel polyoxometalate-based metal organic framework (POMOF) constructed from isolated isopolyoxotungstate $[H_2W_{11}O_{38}]^{8-}$ (abbreviated as $\{W_{11}\}$) clusters and Cu(II) complex cations was achieved, exhibiting an open-framework assembly with one-dimensional (1D) channels. $\{[Cu_2(bpy)(H_2O)_{5.5}]_2[H_2W_{11}O_{38}]\cdot 3H_2O\cdot 0.5CH_3CN\}$ (**1**, where bpy = 4,4′-bpydine) represents the first example of POMOF based on isolated $\{W_{11}\}$ clusters and transition metal complexes, as far as we know. Each $\{W_{11}\}$ cluster acts as a hexadentate ligand to coordinate with six copper complex cations nearly in a plane by the terminal or bridging oxygen atoms of a ring of six basal W positions. It is particularly worth mentioning that the $\{W_{11}\}$ clusters are linked by two copper(II) complexes in an end-to-end fashion, in contrast to the reported face-to-face fashion. The resulting POMOF **1** has been successfully applied to prompt the cyanosilylation with excellent conversion effciency through a heterogeneous manner. The study provides a basis for further design of other iso-POT-based POMOFs with distinct structural features and properties.

ASSOCIATED CONTENT

Supporting Information

Tables listing selected bond lengths and angles for **1** and recycling results for catalyst **1**, text describing the location of protons by means of BVS calculations and catalysis details, figures showing PXRD patterns, IR spectra, and the crystal structure of **1** and HPLC chromatograms of the cyanosilylation of aldehyde products in $CDCl_3$, and crystal data in CIF format. This material is available free of charge via the Internet at http://pubs.acs.org.

AUTHOR INFORMATION

Corresponding Authors

*(Q.H.) Tel./Fax: (+86)-378-3886876. E-mail:hdhqx@henu.edu.cn.

*(J.N.) Tel./Fax: (+86)-378-3886876. E-mail:jyniu@henu.edu.cn.

Notes

The authors declare no competing financial interest.

ACKNOWLEDGMENTS

We gratefully acknowledge the financial support from the National Natural Science Foundation of China (NSFC; Grant Nos. 21101055 and U1304201).

REFERENCES

(1) Dolbecq, A.; Dumas, E.; Mayer, C. R.; Mialane, P. *Chem. Rev.* **2010**, *110*, 6009−6048.

(2) Nohra, B.; Moll, H. E.; Albelo, L. M. R.; Mialane, P.; Marrot, J.; Mellot-Draznieks, C.; O'Keeffe, M.; Biboum, R. N.; Lemaire, J.; Keita, B.; Nadjo, L.; Dolbecq, A. *J. Am. Chem. Soc.* **2011**, *133*, 13363−13374.

(3) Corma, A.; García, H.; Llabrés i Xamena, F. X. *Chem. Rev.* **2010**, *110*, 4606−4655.

(4) Sun, C. Y.; Liu, S. X.; Liang, D. D.; Shao, K. Z.; Ren, Y. H.; Su, Z. M. *J. Am. Chem. Soc.* **2009**, *131*, 1883−1888.

(5) Han, Q. X.; He, C.; Zhao, M.; Qi, B.; Niu, J. Y.; Duan, C. Y. *J. Am. Chem. Soc.* **2013**, *135*, 10186−10189.

(6) Song, J.; Luo, Z.; Britt, D. K.; Furukawa, H.; Yaghi, O. M.; Hardcastle, K. I.; Hill, C. L. *J. Am. Chem. Soc.* **2011**, *133*, 16839−16846.

(7) (a) Pope, M. T. *Heteropoly and Isopoly Oxometalates*; Springer-Verlag: New York, 1983. (b) Song, Y. F.; Tsunashima, R. *Chem. Soc. Rev.* **2012**, *41*, 7384−7402.

(8) Gao, J.; Yan, J.; Beeg, S.; Long, D. L.; Cronin, L. *J. Am. Chem. Soc.* **2013**, *135*, 1796−1805.

(9) Zou, C.; Zhang, Z. J.; Xu, X.; Gong, Q. H.; Li, J.; Wu, C. D. *J. Am. Chem. Soc.* **2012**, *134*, 87−90.

(10) Zheng, S. T.; Yang, G. Y. *Chem. Soc. Rev.* **2012**, *41*, 7623−7646.

(11) Yin, P. C.; Li, T.; Forgan, R. S.; Lydon, C.; Zuo, X. B.; Zheng, Z. N.; Lee, B.; Long, D. L.; Cronin, L.; Liu, T. B. *J. Am. Chem. Soc.* **2013**, *135*, 13425−13432.

(12) Tian, A. X.; Ying, J.; Peng, J.; Sha, J. Q.; Han, Z. G.; Ma, J. F.; Su, Z. M.; Hu, N. H.; Jia, H. Q. *Inorg. Chem.* **2008**, *47*, 3274−3283.

(13) Goberna-Ferrón, S.; Vigara, L.; Soriano-López, J.; Galán-Mascarós, J. R. *Inorg. Chem.* **2012**, *51*, 11707−11715.

(14) Hao, J.; Xia, Y.; Wang, L. S.; Ruhlmann, L.; Zhu, Y. L.; Li, Q.; Yin, P.; Wei, Y. G.; Guo, H. Y. *Angew. Chem., Int. Ed.* **2008**, *47*, 2626−2630.

dx.doi.org/10.1021/ic5004879 | *Inorg. Chem.* 2014, 53, 6107−6112

(15) Streb, C.; Ritchie, C.; Long, D. L.; Kögerler, P.; Cronin, L. *Angew. Chem., Int. Ed.* **2007**, *46*, 7579−7582.
(16) Ma, F. J.; Liu, S. X.; Sun, C. Y.; Liang, D. D.; Ren, G. J.; Wei, F.; Chen, Y. G.; Su, Z. M. *J. Am. Chem. Soc.* **2011**, *133*, 4178−4181.
(17) Li, J.; Huang, Y.; Han, Q. X. *Chin. J. Struct. Chem.* **2013**, *32*, 1897−1903.
(18) Liu, C.; Luo, F.; Liu, N.; Cui, Y.; Wang, X.; Wang, E. B.; Chen, J. *Cryst. Growth Des.* **2006**, *6*, 2658−2660.
(19) Fang, X. K.; Luban, M. *Chem. Commun. (Cambridge, U. K.)* **2011**, *47*, 3066−3068.
(20) Miras, H. N.; Yan, J.; Long, D. L.; Cronin, L. *Angew. Chem., Int. Ed.* **2008**, *47*, 8420−8423.
(21) (a) Long, D. L.; Abbas, H.; Kögerler, P.; Cronin, L. *J. Am. Chem. Soc.* **2004**, *126*, 13880−13881. (b) Long, D. L.; Brucher, O.; Streb, C.; Cronin, L. *Dalton Trans.* **2006**, 2852−2860.
(22) Yan, J.; Long, D. L.; Wilson, E. F.; Cronin, L. *Angew. Chem., Int. Ed.* **2009**, *48*, 4376−4380.
(23) Ismail, A. H.; Dickman, M. H.; Kortz, U. *Inorg. Chem.* **2009**, *48*, 1559−1565.
(24) Yao, S.; Wu, H. L.; Lei, Z. Q.; Yan, J. H.; Wang, E. B. *Chin. Chem. Lett.* **2013**, *24*, 283−286.
(25) Ismail, A. H.; Bassil, B. S.; Suchopar, A.; Kortz, U. *Eur. J. Inorg. Chem.* **2009**, 5247−5252.
(26) Ginsberg, A. P. *Inorganic Syntheses*; John Wiley & Sons: New York, 1990; Vol. *27*, pp 81−82.
(27) *SMART*, Data collection software (version 5.629); Bruker AXS: Madison, WI, USA, 2003.
(28) *SAINT, Data reduction software* (version 6.45); Bruker AXS: Madison, WI, USA, 2003.
(29) Sheldrick, G. M. *SHELXTL97, Program for Crystal Structure Solution*; University of Göttingen: Göttingen, Germany, 1997.
(30) Data for $C_{40}H_{46}N_{12}O_{36}W_{10}Zn$: Tetragonal, space group *P*4(3)2(1)2, a = 13.6803(14) Å, b = 13.6803(14) Å, c = 33.972(4) Å, $\alpha = \beta = \gamma$ = 123.992(3)°.
(31) Data for $C_{10}H_{10}N_2O_{41}W_{12}Zn_2$: Monoclinic, space group *P*2(1)/*c*, a = 13.2094(9) Å, b = 22.3720(15) Å, c = 23.6273(13) Å, β = 123,992(3)°.
(32) Brown, I. D.; Altermatt, D. *Acta Crystallogr.* **1985**, *B41*, 244−247.
(33) Lehmann, T.; Fuchs, J. Z. *Z. Naturforsch., B: J. Chem. Sci.* **1988**, *43*, 89.
(34) Piedra-Garza, L. F.; Dickman, M. H.; Moldovan, O.; Breunig, H. J.; Kortz, U. *Inorg. Chem.* **2009**, *48*, 411−413.
(35) Zheng, L. M.; Wang, Y.; Wang, X.; Korp, J. D.; Jacobson, A. J. *Inorg. Chem.* **2001**, *40*, 1380−1385. (b) Zhang, X.; Chen, Q.; Duncan, D. C.; Campana, C.; Hill, C. L. *Inorg. Chem.* **1997**, *36*, 4208−4215. (c) Chen, Q.; Zubieta, J. *Coord. Chem. Rev.* **1992**, *114*, 107−167.
(36) Okun, N. M.; Anderson, T. M.; Hardcastle, K. I.; Hill, C. L. *Inorg. Chem.* **2003**, *42*, 6610−6612.
(37) Arumuganathan, T.; Das, S. K. *Inorg. Chem.* **2009**, *48*, 496−507.
(38) Farha, O. K.; Hupp, J. T. *Acc. Chem. Res.* **2010**, *43*, 1166−1175.
(39) Eddaoudi, M.; Kim, J.; Rosi, N.; Vodak, D.; Wachter, J.; Keeffe, M. O.; Yaghi, O. M. *Science* **2002**, *295*, 469−472.
(40) Spek, A. L. *J. Appl. Crystallogr.* **2003**, *36*, 7−13.
(41) Schlichte, K.; Kratzke, T.; Kaskel, S. *Microporous Mesoporous Mater.* **2004**, *73*, 81−88.
(42) Dang, D. B.; Wu, P. Y.; He, C.; Xie, Z.; Duan, C. Y. *J. Am. Chem. Soc.* **2010**, *132*, 14321−14323.
(43) Han, Q. X.; Ma, P. T.; Zhao, J. W.; Wang, Z. L.; Yang, W. H.; Guo, P. H.; Wang, J. P.; Niu, J. Y. *Cryst. Growth Des.* **2011**, *11*, 436−444.
(44) The molecular size (17.4× 13.8 Å) was calculated by using the program Chem3D.